

COVER PAGE

Document downloaded by @DAEL

Sat Nov 28 09:42:14 2026
For personal use

When automatic English translation is provided, only the original document is authentic.
The EAA cannot be held responsible of any translation error

Bibliographical reference

Acoustic Thermal Boundary Condition on Thin Bodies: Application to Membranes and Fibres, Thomas Lavergne, Nicolas Joly and Stéphane Durand, Acta Acustica **vol. 99** (Number 4), 2013, pp. 524-536

DOI
https://doi.org/10.3813/AAA.918632

Acta Acustica united with Acustica
Vol. 99 (2013) 524 – 536

DOI 10.3813/AAA.918632

Acoustic Thermal Boundary Condition on Thin Bodies: Application to Membranes and Fibres

Thomas Lavergne, Nicolas Joly, Stéphane Durand
LUNAM Université, Université du Maine, UMR CNRS 6613, Laboratoire d'Acoustique de l'Université du Maine (LAUM), Avenue O. Messiaen, 72085 Le Mans cedex 9, France. nicolas.joly@univ-lemans.fr

Summary
Temperature variations associated with acoustic pressure are known to be quasi-adiabatic in the bulk of the fluid and quasi-isothermal at the walls of relatively thick bodies, developing thermal acoustic boundary layers. For thin rigid bodies, of sufficiently small characteristic length, the thermal boundary condition may differ from isothermal condition. The acoustic field, with particle velocity normal to the boundary near the wall, is studied for both plane geometry (a thin membrane) and a cylindrical one (a fibre): thus, avoiding shear viscosity effects, these analytical models focus on thermal boundary layers effects with the thermal conduction inside the solid body and the heat flow between the fluid and the solid both taken into account. For both geometries, the complex local polytropic coefficient, which is related to the complex local compressibility of the fluid, is used to account for the local condition for the fluid in the neighbourhood of the solid-fluid interface inside the thermal boundary layer. Then, to compare the thermal effects implied by each geometry, both the complex local polytropic coefficient (calculated at the wall) and the acoustic specific admittance of the boundary are used to describe the transition between isothermal and adiabatic thermal conditions as a function of the frequency. Results show that the temperature boundary condition depends significantly on the geometry of the solid body. The boundary condition on the surface of a cylinder can differ significantly from an isothermal one, while it remains isothermal on the surface of a plate with the thickness equal to the cylinder diameter. Results would be of interest in several applications involving fibres, and also confirm the isothermal boundary condition commonly used in the literature when considering plane or shell geometries.

PACS no. 43.20.El, 43.20.Hq, 43.35.Ns, 43.55.Ev

1. Introduction

The propagation of acoustic waves in real fluids is known to be associated with small acoustic perturbations, which are described by particle velocity, pressure, density, and quasi-adiabatic temperature variations in the bulk of the fluid. In contrast with this, at the solid boundaries of the fluid domain, quasi-isothermal and no-slip conditions are satisfied, such that acoustic viscous and thermal boundary layers develop. In this intermediate region, the thermodynamic conditions for the fluid are in transitional regime between the isothermal and the adiabatic ones. Because of their major influence on dissipative processes in thermoviscous fluids, these acoustic boundary layers have been widely studied in the literature [1, 2, 3, 4, 5] including applications to thermoacoustics [6, 7, 8], to porous media and meta-materials [9, 10, 11, 12, 13, 14, 15], to metrology [16, 17, 18, 19, 20, 21, 22] and tranducers [23, 24, 25, 26, 27, 28, 29, 30, 31]. Boundary layers effects can be modelled by admittance-like boundary conditions [32, 5, 33] when the field can be locally approximated by plane waves, by effective properties (dynamic bulk modulus and dynamic density) which are widely used in porous media acoustics when the sound wavelength strongly exceeds the characteristic size of the material microstructure (see for example [12, 34, 35, 36]), or by Finite Element modelling [37, 38, 39, 40, 41] when complex geometries are considered.

Focusing on the thermal conditions for gases, the precise quasi-adiabatic conditions in the bulk of the fluid are well known, even when accounting for molecular relaxation processes [5, 38, 42, 43], and the isothermal condition at thick solid boundaries has revealed to be an excellent approximation [44, 45]. Such an isothermal condition at the boundary is due to the high values of thermal capacity and thermal diffusivity of solid materials compared to those of gases, such that only a tiny temperature variation occurs at the solid/fluid interface when heat is exchanged between the gas and the solid body. Such an isothermal condition is however questionable when a small amount of solid matter is implied, as in the devices involving very thin tubes [46], plates or membranes [27, 29, 31, 41] or in porous materials with very thin fibres. In such devices, due to the finite thermal inertia of the solid medium, the

Received 27 June 2012,
accepted 21 April 2013.

© S. Hirzel Verlag · EAA

heat transfer may lead to temperature variation, leading to a thermal boundary condition different from the isothermal one.

The aim of this paper is to investigate the thermal boundary layer and thermal diffusion processes occurring inside 1-dimensional thin bodies (membranes and fibres) in order to check how accurate the isothermal approximation for such small solid bodies can be. The thermal boundary condition and the thermal boundary layer effects are presented using (i) the local polytropic coefficient, in order to describe the transition from the quasi-isothermal condition at the solid-fluid interface to the quasi-adiabatic condition in the bulk of the domain outside the boundary layer, and (ii) the admittance-like boundary condition, which is here extended to the case of cylindrical waves for fibres. After presenting variables and fundamental equations in section 2, analytical solutions are given in section 3 for a plane geometry (a membrane), and in section 4 for a cylindrical one (a fibre). The results for both geometries are then compared and discussed in section 5. Appendices present, respectively, (A1) an analysis of the dynamic compressibility of air in a fibrous material, and a comparison of the present results to the previous ones, obtained by Tarnow [12], and (A2) analytical expressions of the pressure variation showing the existence of a pressure boundary layer, even if this boundary layer effect is absolutely negligible in practice.

2. Assumptions, variables and fundamental equations

To focus the attention on thermal effects associated with acoustics, the following assumptions and conditions are used in the present study:

1. a small acoustic perturbation is considered, so that in the fluid, pressure, temperature, density and particle velocity take, respectively, the following forms:

$$P = P_0 + p', \tag{1a}$$
$$T = T_0 + \tau', \tag{1b}$$
$$\rho = \rho_0 + \rho', \tag{1c}$$
$$\boldsymbol{V} = \boldsymbol{v}' \text{ (no steady flow)}, \tag{1d}$$

   where (P_0, T_0, ρ_0) are the static conditions for the fluid at rest (without steady flow in equation 1d), and (p', τ', ρ', $\boldsymbol{v}'$) are the acoustic perturbations, small enough so that the basic equations can be linearised as expressed in section 2.2,
2. harmonic movement is assumed, with time factor $e^{i\omega t}$, allowing to benefit from complex notations (symbols for the real part and harmonic time factor are omitted from section 3),
3. the fluid is assumed compressible (adiabatic sound speed c_0, increase in pressure per unit increase in temperature at constant volume $\hat{\beta}$), viscous (shear and bulk viscosity μ and η respectively) and thermally conductive (thermal conductivity λ, heat capacity per unit mass at constant volume c_v, heat capacity per unit mass at constant pressure c_p, adiabatic constant $\gamma = c_p/c_v$),
4. the solid (subscript "w" denoting a wall) is thermally diffusive (its thermal properties are described by the coefficient of thermal conductivity λ_w, the density ρ_w and the heat coefficient per unit of mass c_w) and is assumed to be perfectly rigid, with constant density and without strain, such that the temperature is defined in the solid phase, in a similar form to (1b), with T_0 being a constant in time and space for both fluid and solid phases:

$$T_w = T_0 + \tau'_w, \tag{1e}$$

5. to clearly investigate thermal effects in the boundary layers only, the acoustic movement is selected to avoid any shear effect and any development of viscous boundary layers: normally incident plane waves are assumed for a plane geometry (section 3), and the cylindrical ones are considered for a cylindrical geometry (section 4).

Conditions 5 for the present study are obviously very rare in practical situations (especially the cylindrical waves), in practical applications it is often necessary to consider additional shear viscous movement and viscous boundary layers effects for solutions in thermoviscous fluid. The analytical solutions presented in this paper hide shear viscosity effects, but account for bulk viscosity. The results for thermal effects are obtained with no additional approximation, giving the full coupled solution for the curl-free component of the particle velocity which is relevant to analyse thermal effects. Possible shear viscosity effects, linked to the divergence-free component, are uncoupled from the following solutions, and can simply be added [3, 5], without disturbing the thermal field.

Considering large fluid domains, small acoustic perturbation, and harmonic movement, the boundary conditions used below assume the continuity of the particle velocity (no-slip condition) and the continuity of temperature at the solid-fluid interface; such continuity conditions would not apply for micropores or rarefied gases [34] or considering nonlinear effects at higher amplitudes [47].

2.1. Heat diffusion equation in a rigid solid at rest

In the solid medium the temperature variation $\tau'_w = \tau_w\, e^{i\omega t}$ is governed by the heat conduction equation

$$(i\omega - \xi_w \Delta)\, \tau_w = 0, \tag{2}$$

where $\xi_w = \lambda_w/(\rho_w c_w)$ is the thermal diffusivity of the solid material. The heat flow density $\boldsymbol{\Phi}'_w$ through a solid-fluid interface is given by

$$\boldsymbol{\Phi}'_w = -\lambda_w \mathbf{grad}\, \tau'_w. \tag{3}$$

2.2. Coupled equations and boundary conditions for the acoustic field in thermoviscous fluid at rest

Combining the Stokes-Navier equation, the conservation of mass equation and the conservation of energy equation, and choosing to express all thermodynamic quantities with

the variables p' and τ' only, leads to the following coupled equations [44, 39] involving the particle velocity $\boldsymbol{v}'$ and the temperature variation τ'

$$\omega^2\,\boldsymbol{v}' + (\frac{c_0^2}{\gamma} + \mathrm{i}\omega c_0 \ell_v)\,\mathbf{grad}\,\mathrm{div}\,\boldsymbol{v}' - \mathrm{i}\omega c_0 \ell_v'\,\mathbf{curl\,curl}\,\boldsymbol{v}' - \mathrm{i}\omega\frac{\hat{\beta}}{\rho_0}\mathbf{grad}\,\tau' = \mathbf{0}, \quad (4)$$

$$\mathrm{i}\omega\tau' - \gamma\ell_h c_0\,\mathrm{div}\,\mathbf{grad}\,\tau' + \frac{\gamma-1}{\gamma\hat{\beta}}\rho_0 c_0^2\,\mathrm{div}\,\boldsymbol{v}' = 0, \quad (5)$$

where $\ell_v = (\eta + \frac{4}{3}\mu)/(\rho_0 c_0)$ and $\ell_v' = \mu/\rho_0 c_0$ are the viscous characteristic length, $\ell_h = \lambda_h/(\rho_0\, c_0\, c_p) = \xi/c_0$ the thermal characteristic length and $\xi = \lambda_h/(\rho_0 c_p)$ the thermal diffusivity of the fluid. Note that, according to condition 5 mentioned above, the shear component $\mathbf{curl\,curl}\,\boldsymbol{v}'$ of equation (4) vanishes in the configurations studied in the following sections.

Thereafter, any variable can be expressed using variables τ' and $\boldsymbol{v}'$, such as for example the total pressure variation which is given by

$$\mathrm{i}\omega p' = -\frac{\rho_0 c_0^2}{\gamma}\mathrm{div}\,\boldsymbol{v}' + \mathrm{i}\omega\hat{\beta}\tau', \quad (6)$$

and the density variation which is given by the conservation of mass equation

$$\mathrm{i}\omega\rho' = -\rho_0 \mathrm{div}\,\boldsymbol{v}'. \quad (7)$$

As long as shear viscosity effect is avoided ($\mathbf{curl\,curl}\,\boldsymbol{v}'$ vanishes in equation 4), this formulation leads to solutions which involve acoustic components (subscript a) and entropic components (subscript h)[5, 3]:

$$\tau' = \tau_a' + \tau_h', \qquad \boldsymbol{v}' = \boldsymbol{v}_a' + \boldsymbol{v}_h', \quad (8)$$

where the entropic components have very low amplitudes in comparison with those of the acoustic components in the bulk of the fluid, but the same order of magnitude as the acoustic ones in the neighbourhood of the solid-fluid boundary, *i.e.* inside the thermal boundary layers, whose thickness is given by $\delta_h = \sqrt{2}/|k_h|$ (where k_h is the entropic complex wavenumber which is defined below in section 3 eq. 14b).

Thereafter, the following conditions are assumed at the solid-fluid boundaries:
(i) the particle velocities satisfy the no-slip condition, namely

$$\boldsymbol{v}' = 0 \text{ for a rigid boundary},$$

(ii) the continuity of the temperature variations implies

$$\tau' = \tau_w',$$

and (iii) the continuity of the normal heat flux densities implies

$$\phi' = \phi_w',$$

where ϕ_w' and ϕ' are, respectively, the normal components of the heat flux density in the solid and in the fluid (the heat flux density in the fluid being given by $\boldsymbol{\Phi}' = -\lambda\,\mathbf{grad}\,\tau'$).

2.3. Complex local polytropic coefficient of the fluid

Acoustic propagation involves the compressibility of the fluid, where the thermodynamic conditions for the acoustic perturbation (equations 1a–1d) are known to be quasi-isothermal at the solid-fluid interface, quasi-adiabatic in the bulk of the fluid and far from boundaries, and in transitional conditions between isothermal and adiabatic inside the thermal boundary layer. To depict such isothermal-to-adiabatic thermodynamic conditions for a small, linearised acoustic perturbation (p', τ', ρ', $\boldsymbol{v}'$), we use the local polytropic coefficient of the fluid n, which is defined such as

$$P/\rho^n = C, \quad (9)$$

where C remains constant with respect to time during the thermodynamic process. For isothermal processes in an ideal gas the polytropic coefficient is equal to unity and the compressibility of the gas is $\chi_T = 1/\rho_0\left[\partial\rho/\partial P\right]_{T_0}$. When the process is adiabatic, the polytropic coefficient equals to $\gamma = c_p/c_v$ so that the compressibility of the gas is $\chi_S = \chi_T/\gamma$. In such isothermal or adiabatic conditions, pressure variation is in-phase with the density variation, giving real local compressibility and real local polytropic coefficient.

Inside the thermal boundary layers, for the small linearised acoustic perturbation (p', τ', ρ', $\boldsymbol{v}'$) (equations 1a–1d), thermodynamic process is polytropic in intermediate conditions between isothermal and adiabatic. The local compressibility of the fluid is

$$\chi = \frac{1}{\rho_0}\frac{\rho'}{p'}, \quad (10)$$

where pressure variation (given by equation 6) and density variation (given by equation 7) are shifted in phase, giving complex local compressibility and complex local polytropic coefficient.

In the following sections the complex local polytropic coefficient n is used to describe the local thermodynamic condition for the perturbation of the fluid. This dimensionless coefficient is defined as the ratio of the isothermal compressibility χ_T and the local compressibility χ. Combining the conservation of mass and equation (6), the polytropic coefficient can be written as

$$n = \frac{\chi_T}{\chi} = 1 + \frac{\hat{\beta}\gamma}{c_0^2}\frac{\tau'}{\rho'}. \quad (11)$$

The complex local polytropic coefficient presents the following properties:

1. it is a real number which is equal to unity for local isothermal conditions,
2. it is a real number which is equal to $\gamma = c_p/c_v$ for local adiabatic conditions,
3. its zero phase (when it is a real number) reveals local in-phase pressure and density variations, without power loss (isentropic movement),
4. other complex values with non-zero phase figure local dissipative and irreversible processes due to thermal conduction or bulk viscosity.

Note that, thereafter, symbols both for the real part and for the harmonic time factor are omitted, and that the complex amplitudes (τ_w, ϕ_w, τ, ϕ, V) of, respectively, the temperature variation (τ'_w) and the normal component of the heat flux density ($\mathbf{\Phi}'_w$) in the solid, the temperature variation (τ') and the normal component of the heat flux density ($\mathbf{\Phi}'$), and the particle velocity ($\boldsymbol{v}'$) in the fluid are used.

3. Plane geometry: a thin rigid thermally diffusive membrane

The first geometry considered is a membrane (a rigid plane wall) of finite thickness e which is placed between two semi-infinite domains of the same fluid. The cartesian coordinate system used has its origin O at the top boundary and the Oy-axis is perpendicular to the wall, outwardly directed as indicated in Figure 1; the fields depend on variable y only, and the particle velocity has a single component v_y. In the semi-infinite fluid domain $y > 0$ (hereafter denoted by the subscript 1), the acoustic energy is provided by an incident plane wave, normally at the boundary, as shown in Figure 1. A part of the acoustic energy of the incident wave is reflected in the form of a plane wave which propagates away from the boundary along the y-axis. Temperature variations associated with the acoustic movement in the fluid domain 1 ($y > 0$) give rise to a temperature variation inside the wall which diffuses into the solid domain $0 > y > -e$ (subscript w) towards the bottom boundary at $y = -e$. At this boundary ($y = -e$) the entropic processes give rise to a transmitted acoustic wave which propagates in the semi-infinite fluid domain $-e > y$ (denoted by the subscript 2).

3.1. Solutions for the heat diffusion in the solid

In the solid medium, the amplitude τ_w of the temperature variation τ'_w, which is the solution of the heat conduction equation (2), takes the following form:

$$\tau_w(y) = \tau_{w_1} \cos(k_w y) + \tau_{w_2} \sin(k_w y), \tag{12a}$$

and the amplitude ϕ_w of the normal component of heat flow density $\mathbf{\Phi}_w$, solution of equation (3), is

$$\phi_w(y) = -\lambda_w k_w \tau_w(y), \tag{12b}$$

where $k_w = \sqrt{-\mathrm{i}\omega/\xi_w}$ is the wave number associated with the thermal diffusion, and where τ_{w_1} and τ_{w_2} are arbitrary constants.

3.2. Solutions for the acoustic field in the fluid

In the fluid medium, the complex amplitude $V(y)$ of the y-component of the particle velocity $\boldsymbol{v}'$ and the amplitude $\tau(y)$ of the temperature variation τ', which are solutions of the coupled equations (4–5), are

$$V_{1,2}(y) = \mathrm{i}k_h \left(C^+_{h_{1,2}} \mathrm{e}^{\mathrm{i}k_h y} - C^-_{h_{1,2}} \mathrm{e}^{-\mathrm{i}k_h y} \right) + \mathrm{i}k_a \left(C^+_{a_{1,2}} \mathrm{e}^{\mathrm{i}k_a y} - C^-_{a_{1,2}} \mathrm{e}^{-ik_a y} \right), \tag{13a}$$

$$\tau_{1,2}(y) = C_1 \left(C^+_{h_{1,2}} \mathrm{e}^{\mathrm{i}k_h y} + C^-_{h_{1,2}} \mathrm{e}^{-\mathrm{i}k_h y} \right) + C_2 \left(C^+_{a_{1,2}} \mathrm{e}^{\mathrm{i}k_a y} + C^-_{a_{1,2}} \mathrm{e}^{-\mathrm{i}k_a y} \right), \tag{13b}$$

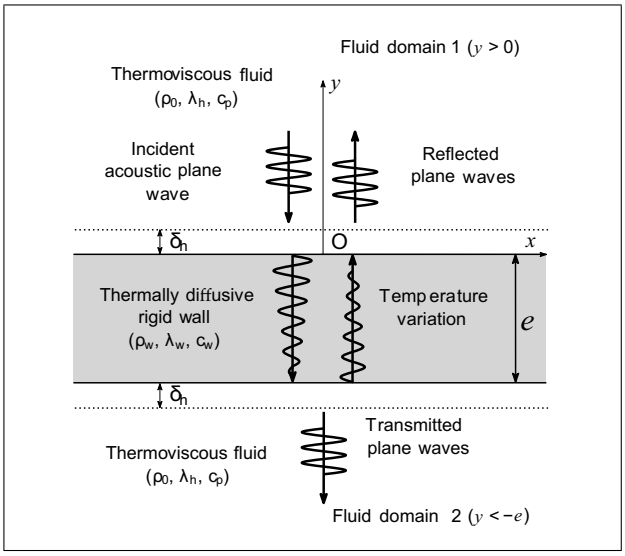

Figure 1. Rigid wall of thickness e inserted between two semi-infinite fluid domains.

where $C^+_{a_{1,2}}$, $C^-_{a_{1,2}}$, $C^+_{h_{1,2}}$ and $C^-_{h_{1,2}}$ are arbitrary constants associated with the acoustic (subscript a) and entropic (subscript h) movements along the positive and negative directions of y-axis (exponents $-$ and $+$ respectively) in the fluid domain 1 (subscript 1) and the fluid domain 2 (subscript 2), C_1 and C_2 are [44] two coefficients given by

$$C_1 = \frac{(H+G)/2Q + \omega^2}{D}, \quad C_2 = \frac{(H-G)/2Q + \omega^2}{D}, \tag{14a}$$

k_a and k_h are the acoustic and entropic wave numbers, respectively, given by

$$\mathrm{i}k_h = \sqrt{\frac{H+G}{2BQ}}, \quad \mathrm{i}k_a = \sqrt{\frac{H-G}{2BQ}}, \tag{14b}$$

with

$$B = c_0^2/\gamma + \mathrm{i}\omega c_0 l_v, \quad D = \mathrm{i}\omega\hat{\beta}/\rho_0, \tag{14c}$$

$$Q = -\gamma l_h c_0, \quad R = -\frac{\gamma - 1}{\gamma\hat{\beta}}\rho_0 c_0^2, \tag{14d}$$

$$H = DR - Q\omega^2 - \mathrm{i}\omega B, \tag{14e}$$

and $$G = \sqrt{H^2 - 4\mathrm{i}\omega^3 BQ}. \tag{14f}$$

The eight constants $C^{\pm}_{a,h_{1,2}}$ (equations 13a and 13b) for the solutions in the fluid domains 1 ($y > 0$) and 2 ($y < -e$), and the two constants $\tau_{w_{1,2}}$ (equation 12a) for the solutions in the solid domain are obtained from the following conditions for the incident waves and the boundary conditions at $y = 0$ and $y = -e$.

3.3. Conditions-related solutions for the fluid domains

In fluid medium 1 ($y > 0$), the solutions V_1 and τ_1 are required to satisfy the following conditions: (i) the acoustic component of the incident wave is chosen equal to unity ($C^+_{a_1} = 1$) (thus the acoustic component of the reflected

wave $C_{a_1}^-$ corresponds to the reflection coefficient R_a in the fluid domain 1), (ii) the entropic component of the incident wave vanishes ($C_{h_1}^+ = 0$). In the fluid domain 2 ($y < -e$), there is no incident wave propagating in the positive y-direction, therefore both the acoustic component and the entropic component vanish ($C_{a_2}^- = C_{h_2}^- = 0$) in the solutions V_2 and τ_2. These conditions for incident waves finally give four of the ten constants cited above.

The six other constants are obtained from the following boundary conditions at the two solid-fluid interfaces:
(i) the particle velocities $\boldsymbol{v}'_{1,2} = V_{1,2}\mathrm{e}^{\mathrm{i}\omega t}$ satisfy the no-slip condition, namely

$$V_1(y=0) = 0 \quad \text{and} \quad V_2(y=-e) = 0,$$

(ii) the continuity of the temperature variations implies

$$\begin{aligned} &\tau_1(y=0) = \tau_w(y=0) \\ \text{and} \quad &\tau_2(y=-e) = \tau_w(y=-e), \end{aligned}$$

and (iii) the continuity of the normal heat flux densities implies

$$\begin{aligned} &\phi_1(y=0) = \phi_w(y=0) \\ \text{and} \quad &\phi_2(y=-e) = \phi_w(y=-e). \end{aligned}$$

Then, the amplitudes of the acoustic and entropic components of the reflected wave (fluid 1), $C_{a_1}^-$ and $C_{h_1}^-$, are

$$C_{a_1}^- = \frac{C_1 N_a L \cos(k_w e) + \left[L^2 - M^2\left(1 + \frac{N_h C_2}{M}\right)\right]\sin(k_w e)}{2LM\cos(k_w e) + \left(L^2 - M^2\right)\sin(k_w e)}, \tag{15a}$$

$$C_{h_1}^- = \frac{-C_2 N_a \left[L\cos(k_w e) - M\sin(k_w e)\right]}{2LM\cos(k_w e) + \left(L^2 - M^2\right)\sin(k_w e)}, \tag{15b}$$

where C_1 and C_2 are given by equation (14a) and the amplitude of the acoustic and entropic components of the transmitted wave (fluid 2), $C_{a_2}^+$ and $C_{h_2}^+$, are

$$C_{a_2}^+ = \frac{-C_2 N_h L \mathrm{e}^{\mathrm{i}k_a e}}{2LM\cos(k_w e) + \left(L^2 - M^2\right)\sin(k_w e)}, \tag{16a}$$

$$C_{h_2}^+ = \frac{C_2 N_a L e^{\mathrm{i}k_h e}}{2LM\cos(k_w e) + \left(L^2 - M^2\right)\sin(k_w e)}, \tag{16b}$$

where

$$\Lambda = \lambda_w/\lambda, \quad N_a = 2\Lambda k_w \mathrm{i}k_a, \tag{17a}$$

$$N_h = 2\Lambda k_w \mathrm{i}k_h, \quad L = \mathrm{i}k_h \mathrm{i}k_a\left(C_1 - C_2\right), \tag{17b}$$

$$M = 1/2\left(N_a C_1 - N_h C_2\right). \tag{17c}$$

It is worth noting that the analytical expression for the pressure variation in the fluid domain 1 involves a pressure boundary layer due to the entropic component (see Appendix A2). This boundary layer can however be neglected, and the total pressure variation can be considered as equal to its acoustic component.

3.4. Complex local polytropic coefficient near the boundary

The numerical results presented in this paper are obtained considering glass as a solid medium ($\rho_w = 2500$ kg.m^{-3}, $\lambda_w = 1$W.m^{-1}.K^{-1}, $c_w = 720$ J.kg^{-1}.K^{-1}) and air as a fluid medium ($\rho_0 = 1.2$ kg.m^{-3}, $\lambda = 0.024$ W.m^{-1}.K^{-1}, $c_p = 1.01 \times 10^3$ J.kg^{-1}.K^{-1}, $\gamma = c_p/c_v = 1.405$, $\hat{\beta} = 347$ kg.m^{-1}.s^{-2}.K^{-1}, $\mu = 1.6910^{-5}$ Pa.s, $c_0 = 344$ m.s^{-1}), but the formulation presented in the previous section can be applied to any fluid and rigid solid (as long as the assumptions and conditions listed in section 2 are satisfied).

Figures 2a and 2b show the real and imaginary parts of the complex polytropic coefficient n (equation 11) in the fluid domain ($y > 0$) as functions of the distance from the boundary, the unit length being the thermal boundary layer thickness δ_h, for two frequencies (10 Hz, Figure 2a, and 10 kHz, Figure 2b) and for several thicknesses of a glass wall. The real part of n depicts the transition between the condition at the boundary (unity for isothermal condition) and the adiabatic condition in the bulk of the fluid [i.e. $\Re(n) = \gamma$]. The imaginary part of n gives information about the phase shift between the density variation and the pressure variation, showing the transition which takes place close to the wall, within a layer with thickness 4 δ_h. The dotted lines ($e = \infty$) in Figures 2a and 2b represent the polytropic coefficient when considering a wall of infinite thickness calculated with the modelling [44].

At 10 Hz (Figure 2a) and for a thickness of the glass wall larger than 5 μm, the dissipation takes place within the thermal boundary layers and the thermal boundary condition can be considered as a quasi-isothermal one (i.e. $\tau_1 = \tau_w = 0$). When considering thinner membranes, the heat transfer leads to a temperature variation, due to the finite thermal inertia of the solid medium, giving a thermal boundary condition slightly different from the isothermal one. At 10 kHz, this phenomenon does not happen and the thermal boundary condition is quasi-isothermal, whatever the thickness of the wall. According to this quasi-isothermal condition on the membrane, including the case of very thin walls, the acoustic wave transmitted in fluid domain two (see Figure 1) by thermal diffusion is totally negligible relative to the mechanical wave transmission that will occur.

4. Cylindrical geometry: a thin rigid thermally diffusive fibre

The second geometry considered is a circular fibre whose diameter D_1 (radius R_1) is assumed to be much smaller than the acoustic wavelength $\Re(2\pi/k_a)$ in the thermo-viscous fluid which surrounds it. The geometry of the problem involves a cylindrical coordinate system (r, θ, z), which has its origin O at the centre of the fibre. Cylindrical incident waves, which provide the acoustic energy, propagate along the radial $r-$axis in the fluid domain $r > R_1$ towards the solid-fluid interface, in such a way that the coordinates θ and z are not involved in the problem and the

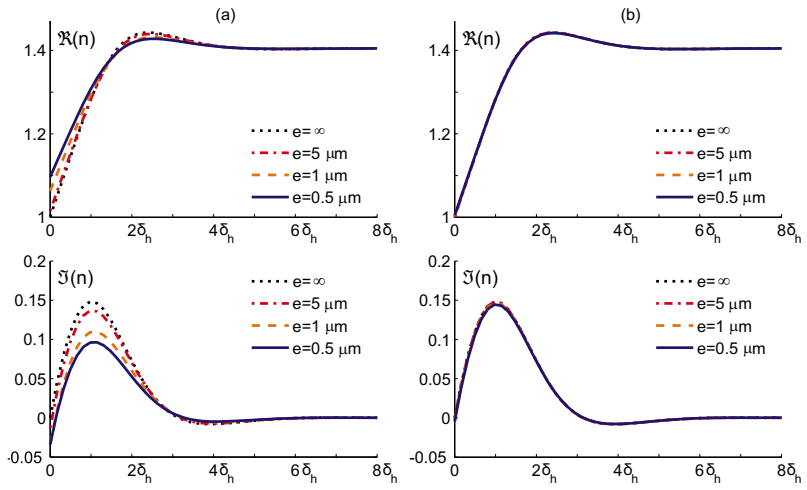

Figure 2. Real part (upper graphs) and imaginary part (lower graphs) of the polytropic coefficient in the fluid domain 1 (air) versus the distance from boundary, scaled by the thermal acoustic boundary layer thickness δ_h, for several thicknesses of a glass membrane (a) at 10 Hz and (b) at 10 kHz.

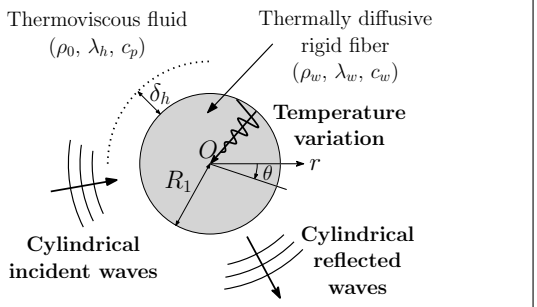

Figure 3. Circular rigid fibre of radius R_1 surrounded by a thermoviscous fluid.

particle velocity $\boldsymbol{v}'$ is radial with the only component v'_r (see Figure 3). The cylindrical reflected waves consist of an acoustic component with amplitude C_a^- and an entropic component with amplitude C_h^-, which is due to the heat diffusion effects in the fluid at the boundary $r = R_1$, giving also rise to thermal diffusion inside the fibre.

4.1. Solution for the heat diffusion in the solid

In the solid medium ($0 < r < R_1$), considering both the geometry of the system and the Neumann condition $\left.\frac{\partial \tau'_w}{\partial r}\right|_{r=0} = 0$ (i.e. finite value of temperature variation at the centre of the fibre), the amplitude τ_w of the temperature variation τ'_w solution of equation (2) is

$$\tau_w = A_w J_0 (k_w r) , \tag{18a}$$

where A_w is an arbitrary constant, $k_w = \sqrt{-i\omega/\xi_w}$ the wavenumber for the thermal diffusion, and J_0 the Bessel function of the first kind of order zero. The heat flux density ϕ_w through the interface is

$$\phi_w = -k_w A_w J_1 (k_w r) , \tag{18b}$$

where J_1 is the Bessel function of the first kind of order one.

4.2. Solutions for the acoustic field in the fluid

In the fluid medium, considering that only the variable r is involved in the problem, the complex amplitude τ_1 of the temperature variation τ'_1 and the complex amplitude V_1 of the r-component of the particle velocity v'_1 in the fluid ($r > R_1$), which are solutions of the coupled equations (4) and (5), are

$$\begin{aligned}\tau_1 (r) = {} & C_a^+ H_0^{(1)} (k_a r) + C_a^- H_0^{(2)} (k_a r) \\ & + C_h^+ H_0^{(1)} (k_h r) + C_h^- H_0^{(2)} (k_h r) ,\end{aligned} \tag{19a}$$

and

$$\begin{aligned}V_1 (r) = {} & K_1 \left[C_h^+ H_1^{(1)} (k_h r) + C_h^- H_1^{(2)} (k_h r) \right] \\ & + K_2 \left[C_a^+ H_1^{(1)} (k_a r) + C_a^- H_1^{(2)} (k_a r) \right]\end{aligned} \tag{19b}$$

where C_a^+, C_a^-, C_h^+ and C_h^- are arbitrary constants, $H_m^{(1)}$ and $H_m^{(2)}$ are Hankel functions of the first kind (convergent wave) and of second kind (divergent wave) of order m, where k_a and k_h are the acoustic and entropic wavenumbers given by equations (14b), and K_1 and K_2 two coefficients given by

$$K_1 = \frac{\frac{H+G}{2B} + i\omega}{k_h R} , \quad K_2 = \frac{\frac{H-G}{2B} + i\omega}{k_a R} . \tag{20}$$

The five constants [A_w in equation (18a) and $C_{a,h}^{\pm}$ in equations (19a)–(19b)] are obtained from the following conditions for the incident waves and boundary conditions at $r = R_1$.

4.3. Conditions-related solutions for the fluid domain

In the fluid medium ($r > R_1$), the following conditions must be satisfied: (i) given that the fibre is surrounded by an infinite domain of fluid, and that the entropic phenomena occur at the boundary, the entropic component of the convergent waves vanishes ($C_h^+ = 0$), (ii) the acoustic

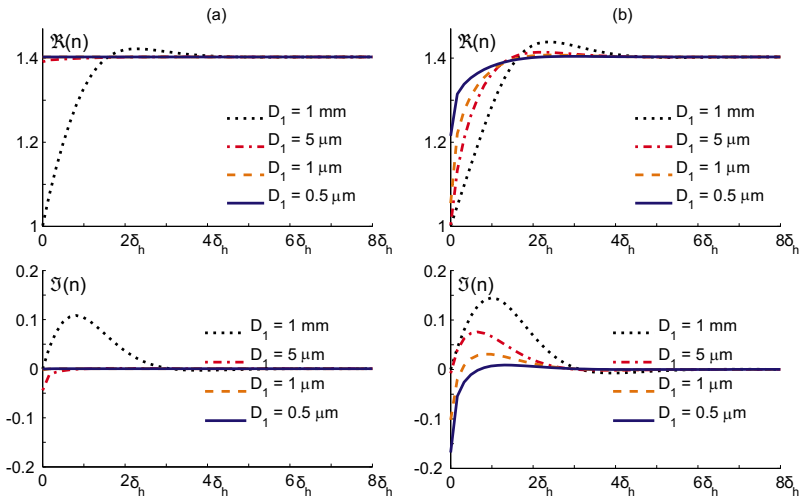

Figure 4. Real part (upper graphs) and imaginary part (lower graphs) of the polytropic coefficient in air versus the distance from boundary, scaled by the thermal acoustic boundary layer thickness δ_h, for different diameters of a glass fibre (a) at 10 Hz and (b) at 10 kHz.

component of the convergent waves is chosen to be equal to unity ($C_a^+ = 1$).

These two conditions for incident waves are completed by the three following boundary conditions at the solid-fluid interface σ_1 ($r = R_1$): (i) the continuity of the temperature variations

$$\tau'_w = \tau'_1,$$

(ii) the continuity of the heat flux densities

$$\phi_w = \phi_1,$$

and (iii) the homogeneous Dirichlet condition for the radial component of the particle velocity at the boundary

$$V_1 = 0,$$

lead to the following expressions of the acoustic and entropic components of the reflected (divergent) waves (Λ is given by equation 17a)

$$C_h^- = \frac{P_{a1}^{(2)} H_0^{(1)}(k_a R_1) - P_{a0}^{(2)} H_1^{(1)}(k_a R_1)}{P_{h1}^{(2)} H_0^{(2)}(k_a R_1) - P_{a1}^{(2)} H_0^{(2)}(k_h R_1) + P_{ha} H_1^{(2)}(k_a R_1)}, \quad (21a)$$

$$C_a^- = \frac{P_{a1}^{(1)} H_0^{(2)}(k_h R_1) - P_{h1}^{(2)} H_0^{(1)}(k_a R_1) + P_{ha} H_1^{(1)}(k_a R_1)}{P_{h1}^{(2)} H_0^{(2)}(k_a R_1) - P_{a1}^{(2)} H_0^{(2)}(k_h R_1) + P_{ha} H_1^{(2)}(k_a R_1)}, \quad (21b)$$

with

$$P_{av}^{(\alpha)} = \Lambda k_w J_1(k_w R_1) H_\nu^{(\alpha)}(k_a R_1) K_2, \quad (22a)$$

$$P_{hv}^{(\alpha)} = \Lambda k_w J_1(k_w R_1) H_\nu^{(\alpha)}(k_h R_1) K_1, \quad (22b)$$

$$P_{ha} = J_0(k_w R_1) H_1^{(2)}(k_h R_1) (K_2 k_h - K_1 k_a), \quad (22c)$$

where α denotes the kind of the Hankel functions (1 or 2) and ν its order (0 up to 2).

It is worth noting that the formulation presented here can be applied to fibrous materials. In Appendix A1, a square lattice of parallel fibres is considered and the results of the dynamic compressibility of the fluid (i.e. the mean value of the compressibility over the whole fluid domain) are compared to those presented in [12].

4.4. Complex local polytropic coefficient near the boundary

Figure 4 shows the real and imaginary parts of the complex polytropic coefficient n in the fluid domain ($r > R_1$) as functions of the distance from the boundary (the unit length being the thermal boundary layer thickness δ_h) at 10 Hz (Figure 4a) and at 10 kHz (Figure 4b) for different diameters of a glass fibre surrounded by air.

At 10 Hz (Figure 4a), and for a radius of the glass fibre smaller than 5 μm, there is no heat transfer between the fibre and the fluid, meaning that the local thermodynamic process for the fluid remains (quasi-)adiabatic: the real part of the complex polytropic coefficient is equal to $\gamma = 1.405$ and its imaginary part vanishes. For a fiber with diameter 5 μm, the real and imaginary parts differ slightly from the (quasi-)adiabatic process showing that a (very) slight heat transfer takes place at the solid-fluid interface. The result obtained for a fiber with diameter 1 mm shows that there is a full heat transfer at the solid-fluid interface leading to the (quasi-)isothermal boundary condition.

At 10 kHz (Figure 4b), the thermal inertia of the fibre is sufficient enough to store the heat by diffusive processes, giving a quasi-isothermal boundary condition for fibre diameters greater than, or equal to 1 μm. It also appears that the fewer the diameter is, the fewer the maximum of $\Re(r)$ is: this is due to the dissipative phenomena which also decrease according to the reduction of the diameter.

5. Plane and cylindrical geometries: comparison of results

In this section, the effects of the thermal boundary layers and their impact on the thermal boundary condition at the solid-fluid interface for both geometries are analysed by using two dimensionless parameters. The first one is the polytropic coefficient of the thermodynamic process calculated at the interface as a function of the frequency for several thicknesses or diameters of the studied solid.

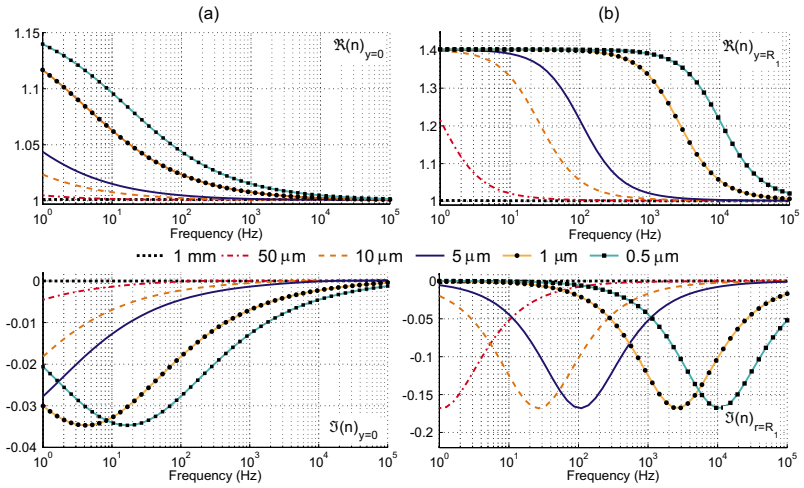

Figure 5. Real part (upper graphs) and imaginary part (lower graphs) of the polytropic coefficient at the solid-fluid interface vs frequency for (a) several thicknesses of membranes and (b) several diameters of fibres.

The second one is the specific admittance of the thermal boundary layers. This dimensionless parameter, defined in section 5.2, turns out to be useful to describe the effects of the thermal boundary layers for the reason that the heat diffusion process acts identically to an additional acoustic admittance of the surface.

5.1. Complex local polytropic coefficient at the solid-fluid interface: Thermal boundary condition as a function of frequency

The thermal boundary condition is evaluated by using the polytropic coefficient n given by equation (11): it is presented in Figure 5a for the plane geometry (section 3) when computed at $y = 0$ for several thicknesses, and in Figure 5b for the cylindrical geometry (section 4) when computed at $r = R_1$ for several diameters. Figure 5 represents the real part (upper graphs) and the imaginary part (lower graphs) of the polytropic coefficient n at the boundary, where, as presented previously, the real part depicts the thermodynamic process which is isothermal when $n = 1$ and adiabatic when $n = \gamma$, and the imaginary part gives information about the phase shift between the density variation and the pressure variation.

As it is shown in Figures 5a and 5b, when considering a thickness (plate) and a diameter (fiber) of 1 mm (dotted lines) the real part of n remains equal to 1 and its imaginary part remains equal to zero in the entire frequency range (1 Hz-100 kHz) meaning that the (quasi-)isothermal boundary condition is valid in both cases. In the case of the plane geometry, the thermal boundary condition remains very close to the (quasi-)isothermal one for a thickness larger than or equal to 5 μm, and differs just slightly from the (quasi-)isothermal one in the lowest frequency range for a thickness smaller than 5 μm. In the case of the cylindrical geometry, the thermal boundary condition differs significantly from the (quasi-)isothermal one, even for diameters between 0.5 μm and 50 μm.

When using the polytropic coefficient at the solid-fluid interface, the different thermal behaviour of thin membranes and fibres can be summarised as follows. On the solid-fluid interface of a membrane, an approximate value of the polytropic coefficient n (11) can be obtained in setting $y = 0$ after substituting the density variation according to mass conservation (7) and solution (V_1, τ_1) (13a, 13b). Taking into account the condition $\Lambda \gg 1$ of a great heat conductivity of the fibre relative to the fluid and removing the negligible terms, this expression can be simplified as (the subscript "—" denotes the plane geometry)

$$n_{_} = \frac{X_{_}}{X_{_} - 1}, \tag{23}$$

with

$$X_{_} = \frac{\gamma}{\gamma - 1}\left(\mathrm{i}k_h\, e\, \kappa + 2\right), \text{ and } \kappa = \frac{\rho_w c_w}{\rho_0 c_p}. \tag{24}$$

Similarly, using solution (19b, 19a) for the fibre, the approximated expression for the polytropic coefficient on the surface of the fibre ($r = R_1$) is (the subscript "•" denotes the cylindrical geometry)

$$n_{\bullet} = \frac{\gamma + X_{\bullet}}{1 + X_{\bullet}}, \tag{25}$$

with

$$X_{\bullet} = -\gamma\, \kappa\, \frac{1 - \mathrm{i}Y_0(k_h R_1)}{1 - 2\mathrm{i}Y_1(k_h R_1)/(k_h R_1)}, \tag{26}$$

where Y_α is the Bessel function of the second kind of order α.

Since $X_{\bullet}$ vanishes as R_1 tends to zero, the polytropic coefficient $n_{\bullet}$ reaches, as expected, the adiabatic value γ for infinitely small diameter of fibre (see figures 4a and 5b at low frequency and for small diameters). In contrast, when considering thin membranes, since the first term in parenthesis in equation (24) vanishes when the thickness e of the membrane tends to zero, the polytropic coefficient $n_{_}$ tends to $2\gamma/(\gamma + 1) \cong 1.17$ for air, that is a good approximation at low frequencies (see figure 2a for a thickness of $e = 0.5\ \mu m$). For non thermal conductive fluids ($\lambda_h = 0$) or large characteristic dimensions (e or R_1) of the solid,

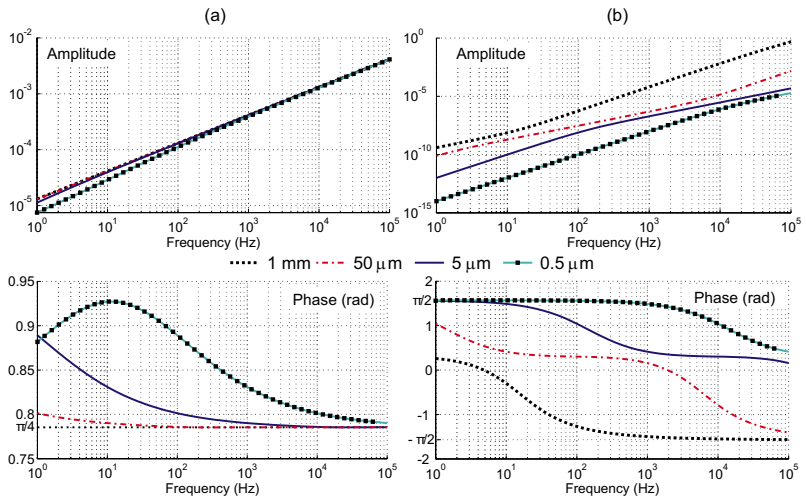

Figure 6. Magnitude (upper graphs) and phase (lower graphs) of the specific acoustic admittance of the boundary layer vs frequency for (a) several thicknesses of glass membranes inserted into air and (b) several diameters of glass fibres.

isothermal condition is reached on the membrane $n_{_} = 1$ whereas the corresponding condition on the fibre is governed by both γ and κ : $n_{\bullet} = \gamma(1-\kappa)/(1-\gamma\kappa)$. More generally, according to approximations (23-26) assuming $\Lambda \gg 1$, the polytropic coefficient at the solid-fluid interface does not depend on the thermal conductivity λ_w of the solid, but depends on the heat capacity ratio κ (24) on the thermal properties of the fluid (γ, k_h), and on the geometry of the solid (e or R_1).

The frequency corresponding to the minimum of the imaginary part of the polytropic coefficient at the boundary matches the central frequency of the transition between isothermal and adiabatic conditions. For instance, on the surface of a membrane, an approximate expression for the transition frequency between isothermal and adiabatic behaviour for the polytropic coefficient $n_{_}$ is

$$f_{_} = \frac{\xi}{2\pi}\left(\frac{\gamma+1}{\gamma\kappa e}\right)^2, \tag{27}$$

illustrated in Figure 5a for the non-isothermal conditions at very low frequencies for very thin membranes.

Such an explicit simple relation for the transition frequency cannot be given from approximate solutions (25-26) for the fibre, instead its value can be obtained numerically using the same criterion.

5.2. Specific acoustic admittance of the thermal boundary layers

When considering a motionless wall, the acoustic boundary admittance is defined as the ratio of the acoustic component of particle velocity $v_{a\perp}$ normal to the solid-fluid interface and the acoustic pressure p at the boundary. The specific (or dimensionless) acoustic admittance β is defined as the product of the acoustic boundary admittance with the characteristic impedance of the fluid (*i.e.* $\rho_0 c_0$). Since the particle velocity $\boldsymbol{v}' = \boldsymbol{v}'_a + \boldsymbol{v}'_h = 0$ vanishes at the interface σ, its acoustic component can be expressed through the entropic one as

$$\beta = \rho_0 c_0 \left.\frac{-v_{h\perp}}{p}\right|_{\sigma}. \tag{28}$$

When the acoustic movement is normal to the boundary, the specific acoustic admittance of the boundary can be expressed directly from the complex reflection coefficient R_a (ratio of the amplitude of the reflected waves over the amplitude of the incident acoustic wave)

$$\beta = \frac{1-R_a}{1+R_a}. \tag{29}$$

It is noteworthy that this last expression is fully valid only assuming local incident *plane* waves *normal* to the boundary, *e.g.* in the case of the plane geometry as the one presented in section 3; however, the same quantity will be plotted here for the cylindrical radial fields presented in section 4 to compare with the thermal effects on a membrane.

Figure 6 shows the magnitude (upper graphs) and the phase (lower graphs) of the specific acoustic admittance β of the boundary layer, for several thicknesses of a glass wall inserted between two semi-infinite fluid domains of air (Figure 6a) and for several diameters of a glass fibre surrounded by air (Figure 6b). In Figure 6a, the upper curve of the magnitude of the admittance β characterizes the quasi-isothermal boundary condition corresponding to an acoustic reflection coefficient very close to unity (this result corresponds to the one presented in [44] for a wall of infinite thickness and for plane waves under normal incidence). When considering a smaller thickness, the admittance β is slightly affected, in the lowest frequency range and at the solid-fluid boundary, due to the heat diffusion in the fluid and in the solid: the magnitude of the admittance β decreases, and the phase shift between the particle velocity and the pressure at the wall deviates slightly from $\pi/4$; the maximum of the phase for a membrane of 5 μm thick seems to be related to the transition between the isothermal and quasi-isothermal boundary condition.

In Figure 6b (for the cylindrical geometry), the heat flux through the solid-fluid interface plays an important role in a wide frequency range, and affects the thermal boundary condition which differs significantly from the isothermal

one for thin fibres of diameters up to several micrometers. On the upper graph, the magnitude of β has a larger dynamic range than the one of the membrane and shows two different slopes; the transition is illustrated by two successive phase shifts, where the first one (at the lower frequency, e.g. for a diameter of 5 μm around 200 Hz) corresponds to the deviation from the isothermal condition (as described by the transition frequency for $n_{\bullet}$ in figure 5b).

6. Conclusion

The analytical modelling of incident harmonic waves normal to the solid-fluid interfaces is useful to focus on the thermal effect to study the thermal boundary condition on the surfaces of thin bodies. When this model is applied to a plane geometry (e.g. a membrane), the results show that the isothermal condition remains valid for a membrane of a thickness of a few micrometers, whereas, when applying the model to a cylindrical geometry (*e.g.* a fibre), the thermal boundary condition differs significantly from the isothermal one for a fibre of similar characteristic dimension. For both geometries, the isothermal boundary condition is a good approximation when the characteristic length of the solid (thickness or diameter) is at least equal to the thermal boundary layer thickness δ_h.

For a fibre with a diameter of a few micrometers, the transition from isothermal boundary condition to the adiabatic one occurs within a narrow frequency bandwidth, whereas, for a membrane of a few micrometers thick, the thermal boundary condition deviates just slightly from the isothermal one.

Applying the model presented in section 2 to a regular square lattice of fibres (appendix A1) leads to the results for the dynamic compressibility of air that are similar to those available in the literature [12].

Appendix

A1. Dynamic compressibility of fibrous materials

Acoustic porous materials are characterized by effective properties including their dynamic compressibility, whose value may depend on the thermal conditions (isothermal to adiabatic) for the fluid. Assuming isothermal condition on the surface of fibres to study the dynamic compressibility of fibrous materials saturated with air is usually a good approximation, except for fibres with very small diameters [12]. Since the thermal conductivity is larger for solids than for gases ($\Lambda = \lambda_w/\lambda_h \gg 1$), more refined models assume non isothermal but time-varying, homogeneous temperature over the section of the fibre (see [12, 36] and [35, appendix B3]).

The aim of this appendix is to link the present local study for polytropic condition inside the fluid with previous works on the compressibility of porous materials, accounting for thermal diffusion inside the solid medium.

The configuration considered here and in references [12, 36] is a fibre of radius R_1 placed in a regular square lattice of periodicity b (see figure A1). Using the formulation presented in sections 4.1 and 4.2, the following model consists of computing the (average) dynamic compressibility $\tilde{\chi}(\omega)$ using equation (10) where the variables ρ' (7) and p' (6) are replaced by their mean values over the total fluid surface of the elementary cell of radius R (see figure A1). Then, the dynamic polytropic coefficient $\tilde{n}(\omega)$ (namely the ratio of the isothermal compressibility over the dynamic compressibility) is compared with the one obtained using the modelling presented by Tarnow in [12] for cylinders placed in a similar, regular square lattice.

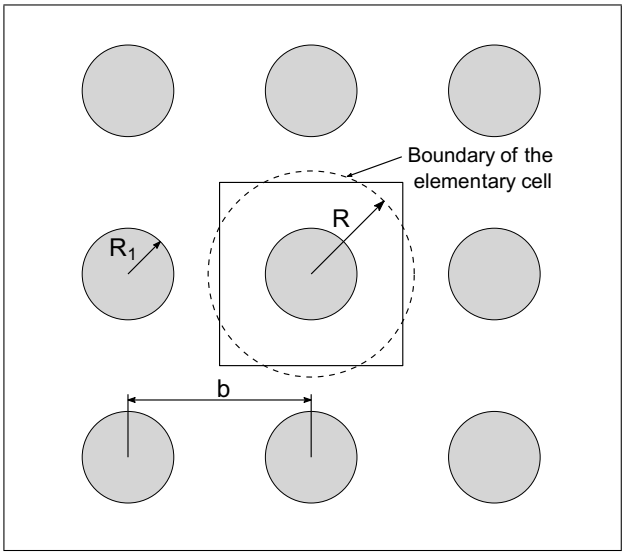

Figure A1. Fibres of radius R_1 placed in a regular square lattice of periodicity b ($\pi R^2 = b^2$).

A1.1. Boundary conditions

The six boundary conditions used in this model are the following ones: according to both the geometry and the symmetry of the solid medium ($0 < r < R_1$), (i) the temperature variation τ'_w satisfies the Neumann boundary condition $\frac{\partial \tau'_w}{\partial r}\Big|_{r=0} = 0$. At the solid-fluid boundary ($r = R_1$) the continuity of (ii) the temperature variations $\tau'_w(r = R_1) = \tau'_1(r = R_1)$, and of (iii) the heat flow densities $\phi_w(r = R_1) = \phi_1(r = R_1)$ are assumed, and (iv) the radial component of the particle velocity satisfies the Dirichlet boundary condition $v'(r = R_1) = 0$. At the boundary of the elementary cell ($r = R$), both (v) the continuity of the temperature variations $\tau'_1(r = R) = \tau'_2(r = R)$, where τ'_2 is the temperature variation outside the elementary cell, and (vi) the Neumann boundary condition $\frac{\partial v'}{\partial r}\Big|_{r=R} = 0$ for the radial component of the particle velocity are satisfied.

A1.2. Tarnow's modelling

The following equations, adapted from the Tarnow's modelling (equations 9–13 in the reference [12]) with the time factor ($e^{i\omega t}$), give the dynamic polytropic coefficient (sub-

script T denoting the use of the Tarnow's modelling)

$$\tilde{n}_T(\omega) = \left[1 - \left(1 - 1/\gamma\right)\left(1 + \frac{2\pi a}{\pi k_h \left(R^2 - R_1^2\right)} \cdot \frac{H_1^1(k_h R)\, J_1(k_h R_1) - H_1^1(k_h R_1)\, J_1(k_h R)}{H_1^1(k_h R)\, J(k_h R_1) - H(k_h R_1)\, J_1(k_h R)}\right)\right]^{-1}, \tag{A1}$$

with

$$J(k_h R_1) = J_0(k_h R_1) - E J_1(k_h R_1), \tag{A2}$$

and

$$H(k_h R_1) = H_0^1(k_h R_1) - E H_1^1(k_h R_1), \tag{A3}$$

where

$$E = \frac{2\lambda k_h}{-i\omega R_1 c_w \rho_w}. \tag{A4}$$

Note that the dynamic polytropic coefficient ($\tilde{n}$) can be expressed in terms of the dynamic compressibility ($\tilde{\chi}$) as follows

$$\tilde{n} = \gamma / \tilde{\chi}. \tag{A5}$$

A1.3. Dynamic polytropic coefficient

Figure A2 represents the real and the imaginary parts of the dynamic polytropic coefficient for a fibrous material with characteristic lengths $R_1 = 3.4\,\mu$m and $b = 75\,\mu$m obtained using the modelling presented in sections 4.1 and 4.2 and the boundary conditions presented in section A1.1 of this appendix (solid line). This result is compared with the modelling presented by Tarnow [12] using equations (A1)–(A4), showing a very good agreement between the two modellings.

A1.4. Influence of heat capacity on the dynamic compressibility of more general porous materials

The model presented in the appendix B3 of reference [35] is capable of predicting the dynamic compressibility of air-filled porous materials, considering more general structures with more complex geometries, but still assuming $\Lambda \gg 1$ and a solid structure composed of small parts separated by a great distance (with geometrical condition similar to the one shown in Figure A1 with $b \gg R_1$). It uses the heat capacity ratio

$$K = \left(\rho_0\, c_p\, \phi_p\right) / \left[\rho_w\, c_w (1 - \phi_p)\right] \tag{A6}$$

of the fluid medium and that of the solid phase, characterized by its porosity ϕ_p and the volume fraction $(1 - \phi_p)$. Note that the parameter K, defined for space averaged properties of porous materials, is similar to the inverse of the heat capacity ratio κ (24) used in above approximations (23-26) on the surface of solids.

In the variable K, the only thermal effect of the solid medium is shown to be its thermal capacity $\rho_w c_w$, which plays an important role in the condition for the space-averaged dynamic compressibility of the porous material at low frequencies given by $(\gamma + K)/(1 + K)$. The frequency dependence of the dynamic compressibility of fibrous materials has been obtained in the work [36], where the precise contribution of the solid thermal inertia over the whole frequency range is taken into account.

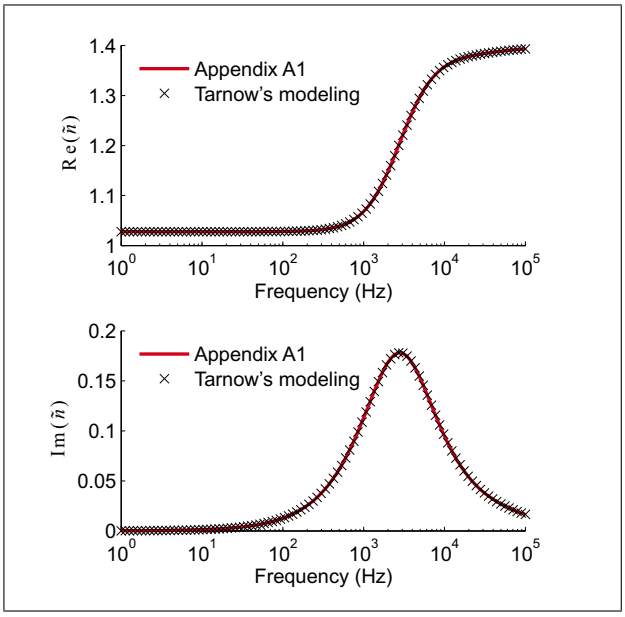

Figure A2. Real and imaginary parts of the dynamic polytropic coefficient for $R_1 = 3.4\,\mu$m and $b = 75\,\mu$m computed with (solid line) the modelling presented in Appendix A1 and (crosses) the Tarnow's modelling [12].

Whereas working with a different variable, namely the local polytropic coefficient on the surface of the fibre, approximate expressions (25,26) for the fibre highlight similar physics, where the thermal behaviour of the solid is governed by the heat capacity of the solid phase (in the ratio κ), that is present in the thermal condition on the surface of thin fibres.

A2. Analytical expression of the pressure boundary layer

The solutions presented in section 3 and 4 give the opportunity to show analytic evidence for pressure boundary layer effects in linear acoustics of thermoviscous fluids, even if their effects are weak enough to neglect them in all practical situations.

Invoking equation 6 and considering harmonic movement allows to express the total pressure variation as the sum of two terms, the first one corresponding to the acoustic component p_a (expressed from the terms of equation (13a) and (13b) associated with the wavenumber k_a), and the second one to the entropic component p_h (terms in (13a) and (13b) associated with the wavenumber k_h):

1. when considering the plane geometry (subscript "—"), invoking equations (13a)–(13b) and considering the boundary conditions enumerated in section 3.3, the total pressure variation (in the fluid domain 1) can be written

as

$$p_{—} = \left(\hat{\beta}C_2 - \frac{\rho_0 c_0^2}{\gamma}\frac{(\mathrm{i}k_a)^2}{\mathrm{i}\omega}\right)\left(\mathrm{e}^{\mathrm{i}k_a y} + C_a^- \mathrm{e}^{-\mathrm{i}k_a y}\right) + \left(\hat{\beta}C_1 - \frac{\rho_0 c_0^2}{\gamma}\frac{(\mathrm{i}k_h)^2}{\mathrm{i}\omega}\right) C_h^- \mathrm{e}^{-\mathrm{i}k_h y}, \quad \text{(A7)}$$

2. when considering the cylindrical geometry (subscript "•"), the equations (19a)–(19b) and the conditions enumerated in section 4.3 lead to the following expression of the total pressure variation

$$p_{\bullet} = \left(\hat{\beta} - \frac{\rho_0 c_0^2}{\gamma}\frac{k_a}{\mathrm{i}\omega}K_1\right)\left(H_0^1(k_a r) + C_a^- H_0^2(k_a r)\right) + \left(\hat{\beta} - \frac{\rho_0 c_0^2}{\gamma}\frac{k_h}{\mathrm{i}\omega}K_2\right) C_h^- H_0^2(k_h r). \quad \text{(A8)}$$

Despite the entropic component of the pressure variation (second terms in equations (A7) and (A8), with wavenuber k_h) is negligible compared to the acoustic component (first terms in equations (A7) and (A8)) in the bulk of the fluid, its (very slight) variation just near the solid-fluid interface involves a pressure boundary layer, for both geometries. The pressure variation caused by the pressure boundary layer effect is obviously insignificant in comparison to the total pressure inside the boundary layer. In air under standard conditions (namely at atmospheric pressure and ambient temperature), the amplitude of the entropic component in the neighbourhood of the solid-fluid interface is approximatively 10^{10} times smaller than the acoustic component at 10 Hz, and 10^7 times smaller at 10 kHz (this ratio decreases as the inverse of frequency). Thus, the assumption that the total pressure is equal to its acoustic component (and therefore neglecting the entropic one) is excellent, even inside the thermal boundary layer.

Acknowledgement

The authors would like to thank D. Lafarge for helpful discussions, and are grateful to the anonymous journal reviewers for providing valuable suggestions which led to improve this paper.

References

[1] G. Kirchhoff: Ueber den Einfluss der Wärmeleitung in einem Gase auf die Schallbewegung. Annalen der Physik **210** (1868) 177–193.

[2] H. Tijdeman: On the propagation of sound waves in cylindrical tubes. J. Sound Vib. **39** (1975) 1–33.

[3] M. Bruneau, P. Herzog, J. Kergomard, J. D. Polack: General formulation of the dispersion equation in bounded visco-thermal fluid, and application to simple geometries. Wave Motion **11** (1989) 441–451.

[4] W. M. Beltman: Viscothermal wave propagation including acousto-elastic interaction. Part I: Theory. J. Sound Vib. **227** (1999) 555–586.

[5] M. Bruneau, T. Scelo: Fundamentals of acoustics. ISTE, 2006.

[6] G. Swift: Thermoacoustic engines. J. Acoust. Soc. Am. **84** (1988) 1145–1180.

[7] N. Rott: Thermoacoustics. Advances in Applied Mechanics **20** (1980) 135–175.

[8] G. Poignand, P. Lotton, G. Penelet, M. Bruneau: Thermoacoustic, small cavity excitation to achieve optimal performance. Acta Acustica united with Acustica **97** (2011) 926–932.

[9] C. Zwikker, C. W. Kosten: Sound absorbing materials. Elsevier, Amsterdam, 1949.

[10] M. R. Stinson, Y. Champoux: Propagation of sound and the assignment of shape factors in model porous materials having simple pore geometries. J. Acoust. Soc. Am. **91** (1992) 685–695.

[11] X. Olny, R. Panneton: Acoustical determination of the parameters governing thermal dissipation in porous media. J. Acoust. Soc. Am. **123** (2008) 814–824.

[12] V. Tarnow: Compressibility of air in fibrous materials. J. Acoust. Soc. Am. **99** (1996) 3010–3017.

[13] H. I. Hussain, J.-L. Guyader: Sound radiation of plates in thermoviscous media. Acta Acustica united with Acustica **95** (2009) 997–1005.

[14] V. Tournat, V. Pagneux, D. Lafarge, L. Jaouen: Multiple scattering of acoustic waves and porous absorbing media. Phys. Rev. E **70** (2004) 1–10.

[15] A. Duclos, D. Lafarge, V. Pagneux: Transmission of acoustic waves through 2d phononic crystal: visco-thermal and multiple scattering effects. Eur. Phys. J. Appl. Phys. **45** (2009) 11302.

[16] J. B. Mehl, M. R. Moldover, L. Pitre: Designing quasi-spherical resonators for acoustic thermometry. Metrologia **41** (2004) 295–304.

[17] M. R. Moldover, J. B. Mehl, M. Greenspan: Gas-filled spherical resonators: Theory and experiment. J. Acoust. Soc. Am. **79** (1986) 253–272.

[18] C. Guianvarc'h, R. Gavioso, G. Benedetto, L. Pitre, M. Bruneau: Characterization of condenser microphones under different environmental conditions for accurate speed of sound measurements with acoustic resonators. Review of Scientific Instrument **80** (2009) 1–10.

[19] C. Guianvarc'h, L. Pitre, M. Bruneau, A.-M. Bruneau: Acoustic field in a quasi-spherical resonator: Unified pertubation model. J. Acoust. Soc. Am. **125** (2009) 1416–1425.

[20] D. Rodrigues, C. Guianvarc'h, J.-N. Durocher, M. Bruneau, A.-M. Bruneau: A method to measure and interpret input impedance of small acoustic components. J. Sound Vib. **315** (2008) 890–910.

[21] P. Honzík, N. Joly, S. Durand, D. Rodrigues, J.-N. Durocher, M. Bruneau: Finite element modelling of acoustic field inside small components: application to an annular slit terminated by an aperture in an infinite screen. Metrologia **49** (2012) 32–40.

[22] C. Guianvarc'h, M. Bruneau: Acoustic fields in binary gas mixtures: mutual diffusion effects throughout and beyond the boundary layers. J. Acoust. Soc. Am. **131** (2012) 4252–4262.

[23] I. B. Crandall: The air-damped vibrating system: theoretical calibration of the condenser transmitter. Physical Review **11** (1918) 449–460.

[24] A. J. Zuckerwar: Theoretical response of condenser microphones. J. Acoust. Soc. Am. **64** (1978) 1278–1285.

[25] Z. Škvor: On acoustical resistance due to viscous losses in the air gap of electrostatic transducers. Acustica **19** (1968) 295–299.

[26] M. Bruneau, A.-M. Bruneau, Z. Škvor, P. Lotton: An equivalent network modelling the strong coupling between a vi-

brating membrane and a fluid film. Acta Acustica **2** (1994) 223–232.

[27] S. Thompson, J. L. LoPresti: Thermal boundary layer effects on the acoustical impedance of enclosures and consequences for acoustical sensing devices. J. Acoust. Soc. Am. **123** (2008) 1364–1370.

[28] P. Honzík, Z. Škvor, S. Durand, M. Bruneau: Electrostatic transducer with square membrane and non-planar back plate: Simplified model. Acta Acustica united with Acustica **95** (2009) 866–873.

[29] T. Le Van Suu, S. Durand, M. Bruneau: Fluid layer trapped between a plane, circular membrane and an axisymmetrically curved, smooth backing wall: analytical model of the dynamic behaviour. Acta Acustica united with Acustica **94** (2008) 474–482.

[30] C. W. Tan, J. Miao: Modified Škvor-Starr approach in the mechanical-thermal noise analysis of condenser microphone. J. Acoust. Soc. Am. **126** (2009) 2301–2305.

[31] T. Lavergne, S. Durand, D. Rodrigues, M. Bruneau, N. Joly: Dynamic behavior of the circular membrane of an electrostatic microphone: Effect of holes in the backing electrode. J. Acoust. Soc. Am. **128** (2010) 3459–3477.

[32] L. Cremer: On the acoustic boundary layer outside a rigid wall. Arch. Elektr. Uebertr. **2** (1948) 136–139.

[33] R. Bossart, N. Joly, M. Bruneau: Hybrid numerical and analytical solutions for acoustic boundary problems in thermo-viscous fluids. J. Sound Vib. **263** (2003) 69–84.

[34] O. Umnova, D. Tsiklauri, R. Venegas: Effect of boundary slip on the acoustical properties of microfibrous materials. J. Acoust. Soc. Am. **126** (2009) 1850–1861.

[35] D. Lafarge, P. Lemarinier, J. F. Allard, V. Tarnow: Dynamic compressibility of air in porous structures at audible frequencies. J. Acoust. Soc. Am. **102** (1997) 1995–2006.

[36] P. Lemarinier: Propagation de son à basses fréquences audibles (30–5000 Hz) dans les mousses et une laine de verre saturées d'air : validation expérimentale de modèles thermiques, analogies diélectriques, imprégnation polymère de mousses. Th. Université du Maine, TH2327, 1997.

[37] C. Karra, M. Ben Tahar: An integral equation formulation for boundary element analysis of propagation in viscothermal fluids. J. Acoust. Soc. Am. **102** (1997) 1311–1318.

[38] R. Christensen, P. Juhl, V. Cutanda Henriquez: Practical modeling of acoustic losses in air due to heat conduction and viscosity. Acoustics 08, Paris, 2008.

[39] N. Joly: Finite element modeling of thermoviscous acoustics on adapted anisotropic meshes: Implementation of the particle velocity and temperature variation formulation. Acta Acustica united with Acustica **95** (2010) 102–114.

[40] W. R. Kampinga, Y. H. Wijnant, A. de Boer: An efficient finite element model for viscothermal acoustics. Acta Acustica united with Acustica **97** (2011) 618–631.

[41] D. Homentcovschi, R. N. Miles: An analytical-numerical method for determining the mechanical response of a condenser microphone. J. Acoust. Soc. Am. **130** (2011) 3698–3705.

[42] J. E. Piercy, T. F. W. Embleton, L. G. Sutherland: Review of noise propagation in the atmosphere. J. Acoust. Soc. Am. **61** (1977) 1403–1418.

[43] M. C. Bérengier, B. Gauvreau, P. Blanc-Benon, D. Juvé: Outdoor sound propagation: A short review on analytical and numerical approaches. Acta Acustica united with Acustica **89** (2003) 980–991.

[44] N. Joly, M. Bruneau, R. Bossart: Coupled equations for particle velocity and temperature variation as the fundamental formulation of linear acoustics in thermo-viscous fluids at rest. Acta Acustica united with Acustica **96** (2006) 202–209.

[45] G. Huelsz, E. Ramos: Temperature measurements inside the oscillatory boundary layer produced by acoustic waves. J. Acoust. Soc. Am. **102** (1998) 1532–1537.

[46] D. H. Keefe: Acoustical wave propagation in cylindrical ducts: Transmission line parameter approximations for isothermal and nonisothermal boundary conditions. J. Acoust. Soc. Am. **75** (1984) 58–62.

[47] O. K. Mawardi: On acoustic boundary layer heating. J. Acoust. Soc. Am. **26** (1954) 726–731.